

Exciton dynamics and random lasing in surface-passivated CdSe/CdSeS core/crown nanoplatelets

Huan Liu(刘欢), Puning Wang(王谱宁), and Rui Chen(陈锐)
Citation: Chin. Phys. B, 2025, 34 (**9**): 094201. DOI: 10.1088/1674-1056/adcd46
http://cpb.iphy.ac.cn; http://iopscience.iop.org/cpb

What follows is a list of articles you may be interested in

Impact of amplified spontaneous emission noise on the SRS threshold of high-power fiber amplifiers

Wei Liu(刘伟), Shuai Ren(任帅), Pengfei Ma(马鹏飞), and Pu Zhou(周朴)
Chin. Phys. B, 2023, 32 (**3**): 034202. DOI: 10.1088/1674-1056/ac833e

Loss prediction of three-level amplified spontaneous emission sources in radiation environment

Shen Tan(谭深), Yan Li(李彦), Hao-Shi Zhang(张浩石), Xiao-Wei Wang(王晓伟), and Jing Jin(金靖)
Chin. Phys. B, 2022, 31 (**6**): 064211. DOI: 10.1088/1674-1056/ac43a8

Pump pulse characteristics of quasi-continuous-wave diode-side-pumped Nd:YAG laser

Zexin Song(宋泽鑫), Qi Bian(卞奇), Yu Shen(申玉), Keling Gong(龚柯菱), Nan Zong(宗楠), Qingshuang Zong(宗庆霜), Yong Bo(薄勇), and Qinjun Peng(彭钦军)
Chin. Phys. B, 2022, 31 (**5**): 054208. DOI: 10.1088/1674-1056/ac447f

Modeling of cascaded high isolation bidirectional amplification in long-distance fiber-optic time and frequency synchronization system

Kuan-Lin Mu(穆宽林), Xing Chen(陈星), Zheng-Kang Wang(王正康), Yao-Jun Qiao(乔耀军), and Song Yu(喻松)
Chin. Phys. B, 2021, 30 (**7**): 074208. DOI: 10.1088/1674-1056/abf105

980-nm all-fiber mode-locked Yb-doped phosphate fiber oscillator based on semiconductor saturable absorber mirror and its amplifier

Ping-Xue Li(李平雪), Yi-Fei Yao(姚毅飞), Jun-Jie Chi(池俊杰), Hao-Wei Hu(胡浩伟), Guang-Ju Zhang(张光举), Bo-Xing Liang(梁博兴), Meng-Meng Zhang(张孟孟), Chun-Mei Ma(马春媚), Ning Su(苏宁)
Chin. Phys. B, 2016, 25 (**8**): 084207. DOI: 10.1088/1674-1056/25/8/084207

SPECIAL TOPIC — Exciton physics: Fundamentals, materials and devices

Exciton dynamics and random lasing in surface-passivated CdSe/CdSeS core/crown nanoplatelets

Huan Liu(刘欢)[†], Puning Wang(王谱宁)[†], and Rui Chen(陈锐)[‡]

Department of Electrical and Electronic Engineering, Southern University of Science and Technology, Shenzhen 518055, *China*

(Received 14 March 2025; revised manuscript received 3 April 2025; accepted manuscript online 16 April 2025)

CdSe nanoplatelets (NPLs) are promising candidates for on-chip light sources, yet their performance is hindered by surface defects and inefficient optical gain. Herein, we demonstrate that CdSeS crown passivation significantly enhances the photophysical property of CdSe NPLs. Laser spectroscopy techniques reveal suppressed electronic and hole trapping at lateral surfaces, leading to a 4.2-fold increase in photoluminescence quantum yield and a shortened emission lifetime from 13.5 to 4.8 ns. In addition, amplified spontaneous emission is achieved under nanosecond pulse pumping, with thresholds of 0.75 to 0.16 mJ/cm^2 for CdSe and CdSe/CdSeS NPLs, respectively. By integrating CdSe/CdSeS NPLs with high-refractive-index SiO_2 scatters, coherent random lasing is realized at a threshold of 0.21 mJ/cm^2. These findings highlight the critical role of lateral surface passivation in optimizing optical gain and pave the way for low-cost, multifunctional nanophotonic devices.

Keywords: CdSe nanoplatelets, core/crown heterostructures, surface passivation, amplified spontaneous emission, random lasing

PACS: 42.62.Fi, 42.55.–f, 61.46.Df

DOI: 10.1088/1674-1056/adcd46 **CSTR:** 32038.14.CPB.adcd46

1. Introduction

Since its invention in the 1960s, the laser has played a pivotal role in various research fields, becoming one of the key technologies driving social and economic development. Over the past 60 years, liquid, solid, gas and semiconductor lasers have matured in their fabrication technologies. Among them, random lasers, a new type of lasers, have attracted significant attention in recent years due to their unique physical properties and potential applications. Compared to traditional lasers, random lasers offer advantages such as tunable coherence, high spatial resolution, multi-peak emission and wide-angle emission, which make them suitable for applications in speckle-free imaging, biosensing, optical display and photonics research.[1–3] In addition, random lasers feature simple structure and relatively straightforward manufacturing process, which reduces cost and complexity, enabling the potential for large-scale application.[4–6] However, the generation mechanism of random lasers differs fundamentally from that of traditional lasers. Instead of relying on resonant cavity feedback, random lasers depend on multiple scattering, making wavelength tunability a major challenge. Traditional lasers can achieve wavelength tuning through optical harmonic generation, but random lasers face difficulties in controlling wavelength in a similar manner due to their multi-peak and wide-angle emission, which limits the optical harmonic generation. Therefore, the development of new gain medium with wavelength tunability, high stability and low cost has become a key focus of random lasers.

Among various semiconductor materials, CdSe colloidal nanocrystals (NCs) have emerged as an ideal candidate for random laser gain medium due to their excellent optical properties and tunable emission characteristics.[4,7–9] In addition, CdSe NCs offer advantages such as simple preparation process, solution processing capability, and high photostability, which make them highly promising for optical gain medium application.[9,10] In particular, CdSe nanoplatelets (NPLs), a specific form of CdSe NCs, are considered one of the most promising optical gain media because of their narrow emission bands, fast photoluminescence (PL) lifetimes, large absorption cross-sections, strong oscillator strengths and low laser thresholds.[11] In addition, the emission wavelength of CdSe NPLs can be precisely controlled by adjusting their thickness and size, which provides a novel solution for achieving wavelength tunability in random lasers.

Although CdSe NPLs show great promise for use in lasers, several challenges remain, particularly in improving the optical gain coefficient and stability. At present, nanoheterojunction is the most effective and common method for passivating surface defects of CdSe NCs. Previous studies on the optical properties of CdSe NCs have demonstrated that the CdSeS alloy shell provides better surface passivation than CdS.[12–14] This is because the alloy shell smooths

[†]These authors contributed equally to this work.

[‡]Corresponding author. E-mail: chenr@sustech.edu.cn

© 2025 Chinese Physical Society and IOP Publishing Ltd. All rights, including for text and data mining, AI training, and similar technologies, are reserved.

the interface barrier of the NCs, thereby enhancing the optical gain properties.[15] In addition, compared to the type-II band structure of CdSe/CdTe, the type-I electronic structure of CdSe/CdS and CdSe/CdSeS has fewer interface defects.[16,17] Due to the unique layered structure of the CdSe NPLs, the passivated vertical (core/shell) and lateral (core/crown) surfaces exhibit distinct optical properties. According to our previous research, passivating the lateral surface can not only improve the optical properties of CdSe, but also preserve its strong quantum confinement effect on the vertical plane, which helps maintain its high optical gain properties.[18] However, the current research on CdSe lateral surface passivation is mostly focused on CdSe/CdS core/crown NPLs prepared by a two-pot method. Poor surface passivation and complex preparation process are not conducive to the application of CdSe NPLs in future optoelectronic devices. Besides, it is a challenge to realize random lasing in NPLs films because films formed by drop-casting or spin-coating of NPLs can only generate amplified spontaneous emission (ASE). Although random lasing has been achieved in CdSe/CdZnS core/shell structures, the quantum confinement effect of CdSe is released on the vertical plane, which limits its wavelength adjustment and is not conducive to the development of blue and green random lasing. Therefore, it is more promising to study the surface passivation and random lasing of CdSe/CdSeS core/crown NPLs prepared by a one-pot method with fewer interface defects. In this work, CdSe and CdSe/CdSeS core/crown NPLs were prepared using a one-pot method. It was found that the photoluminescence quantum yield (PLQY) of CdSe NPLs was improved and the PL lifetime was reduced due to the passivation of lateral surface hole trapping by CdSeS crown. The type-I electronic structure of CdSe/CdSeS was confirmed through transient absorption spectroscopy. At the same time, it was found that CdSe/CdSeS exhibited a slower carrier recovery curve, which confirmed that the electronic trapping on the lateral surface of CdSe NPLs was passivated by CdSeS crown. The ASE threshold of CdSe/CdSeS NPLs was one-fifth that of CdSe NPLs. Furthermore, coherent random lasing action with a threshold of 0.21 mJ/cm^2 was observed.

2. Experimental details

2.1. Synthesis of NPLs

CdSe and CdSe/CdSeS core/crown NPLs were synthesized according to the procedure reported by Hu *et al.* with slight modification.[19] Specifically, 170 mg of cadmium myristic acid, 12 mg of Se powder, and 15 mL of octadecene were put into a 50 mL flask. The solution was degassed for 10 min at 100 °C. When the solution temperature reached 195 °C, 40 mg of cadmium acetate was added to the flask. Subsequently, the solution was reacted at 240 °C for 10 min. The heating stage was removed and the reaction solution was allowed to cool naturally. When the temperature dropped to 160 °C, 2 mL of oleic acid was added as a ligand. To remove H_2S, the solution was degassed at 110 °C for 10 min. When the temperature dropped to 70 °C, 10 mL of *n*-hexane was added to the flask. In order to remove byproducts, the reaction solution was purified at a rate of 7000 rpm. The supernatant was discarded and the precipitate was redispersed in 10 mL of *n*-hexane. Subsequently, 5 mL of acetonitrile and chloroform were added, and the mixture was centrifuged at 5000 rpm. The supernatant was discarded and the precipitate was dispersed in 10 mL of *n*-hexane for optical test. The preparation of CdSe/CdSeS NPLs is similar to that of CdSe NPLs. After the reaction solution reacted at 240 °C for 10 min to form CdSe NPLs, S-ODE was injected into the solution at a rate of 9 mL/h through a syringe pump. The S atoms combined with Cd and Se atoms in the solution to form a CdSeS crown. The purification process of CdSe/CdSeS NPLs is the same as that of CdSe NPLs.

2.2. Structural and optical characterization

Transmission electron microscopy (TEM) images of the CdSe and CdSe/CdSeS NPLs were obtained using a FEI Talos F200X microscope. The linear absorption of the NPLs solutions was measured with a JASCO-1500 spectrometer at room temperature. The PL decay signals were recorded by a fluorescence spectrometer (FS5). The NPLs solution was drop-cast onto a quartz plate to form a dense film, which was then used for ASE and laser measurements. The 800 nm pulse with a repetition rate of 1 kHz and a pulse duration of 100 femtosecond (fs) was generated from a Ti-sapphire laser system (Spectra-Physics) and divided into two parts. One part was coupled an optical parametric amplifier (OPA) to generate pumping pulse and the other part was used to excite a CaF_2 crystal to produce white light. The linear polarization of the pump pulse was adjusted to be perpendicular to that of the probe pulse to eliminate any contribution from coherent artifacts at early times.[16]

3. Results and discussion

The TEM images of 4-monolayer (ML) CdSe and CdSe/CdSeS NPLs are shown in Figs. 1(a) and (1b), respectively. It can be seen that CdSe NPLs exhibit two orientations: face-down and edge-up, which confirms the successful preparation of the NPLs.[20] According to the size statistics, the length and width of CdSe NPLs are 14.7 and 5.8 nm respectively, while for CdSe/CdSeS NPLs, the corresponding values are 24.8 and 10.2 nm.

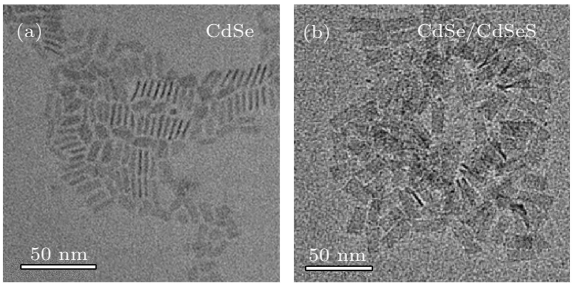


Fig. 1. TEM image of NPLs: (a) CdSe, (b) CdSe/CdSeS.

The normalized UV-visible absorption spectra of CdSe and CdSe/CdSeS NPLs are shown in Fig. 2(a). It can be seen that both NPLs exhibit sharp absorption peaks at 512 and 513 nm, respectively, corresponding to the heavy hole transition.[21] In addition, they show another absorption peak at 485 nm, which is attributed to the light hole transition.[22] At 405 nm, CdSe/CdSeS NPLs exhibit stronger absorption compared to the 4 ML CdSe NPLs, which can be ascribed to the absorption of the CdSeS crown.[23] The normalized PL spectra of CdSe and CdSe/CdSeS NPLs are also shown in Fig. 2(a). It is found that the PLs of CdSe and CdSe/CdSeS NPLs are centered at 512.5 and 513.5 nm, respectively, both with a full width at half-maximum (FWHM) of about 8 nm. The PL peak and FWHM confirm the successful synthesis of 4 ML CdSe NPLs. Although the PL of CdSe NPLs is thickness-dependent, a slight redshift in the emission peak after growing CdSeS crown suggests changes in the dielectric environment and lateral quantum confinement effect.[24,25] The inset of Fig. 2(a) shows the images of CdSe and CdSe/CdSeS NPLs solutions with the same absorbance at 512 nm when illuminated by white (top) and UV (bottom) light. It can be seen that CdSe/CdSeS shows brighter emission than CdSe NPLs. The PLQYs of CdSe and CdSe/CdSeS NPLs were determined to be 19% and 80%, respectively, by integrating sphere. In order to ensure the accuracy of the PLQY results, a 450 nm light source was chosen to excite the CdSe core while CdSeS was not excited. The higher PLQY of CdSe/CdSeS NPLs not only confirms that the passivation of non-radiative recombination centers on the lateral surface of CdSe, but also validates the successful preparation of CdSe/CdSeS core/crown NPLs. Their PL decay traces at room temperature are shown in Fig. 2(b). The average PL lifetimes of CdSe and CdSe/CdSeS NPLs were determined to be 13.5 and 4.8 ns, respectively. According to our previous results, the faster PL decay of CdSe/CdSeS NPLs is attributed to the capture and release of cadmium vacancies.[26] Specifically, a cadmium vacancy of about 19 meV locates on the lateral surface of the CdSe NPLs. When holes are captured by cadmium vacancies, they subsequently escape with the assistance of environmental energy ($\sim$ 26 meV), which results in an additional path for holes before recombination. Therefore, the number of cadmium vacancies and the PL lifetime of the CdSe NPLs are positively correlated. Based on the result, it can be inferred that the cadmium vacancies distributed on the lateral surface of CdSe NPLs are effectively passivated by CdSeS crown.[26]

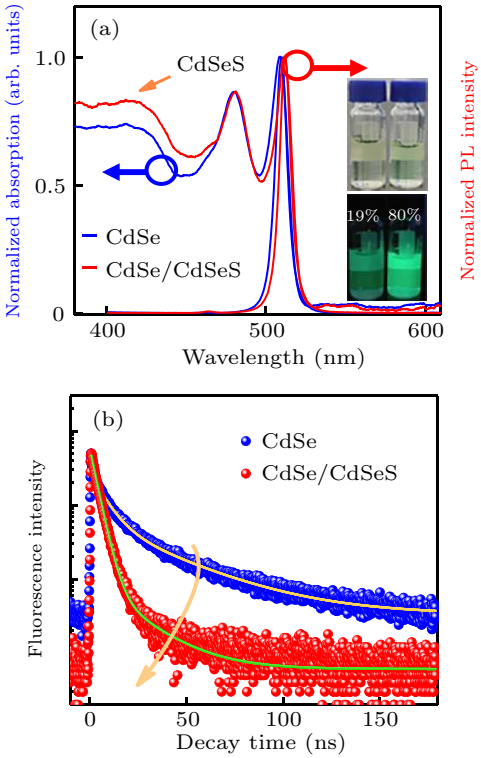


Fig. 2. (a) Normalized absorption and PL spectra of CdSe and CdSe/CdSeS NPLs. The inset is the NPLs solution images under white and UV light. (b) Normalized PL decay curves of CdSe and CdSe/CdSeS NPLs.

In order to further investigate the passivation of the lateral surface of CdSe NPLs, the transient absorption spectra (TAS) of CdSe and CdSe/CdSeS NPLs were measured. The type-I electronic structure of CdSe/CdSeS has been confirmed in our previous research, and the energy band structure is shown in Fig. 3(a).[26] Furthermore, the band gaps of CdSe and CdSeS were determined to be 2.43 and 3.05 eV, respectively. Due to the type-I electronic structure, the electrons and holes generated in CdSeS crown would be transferred to the CdSe core. To prevent carrier migration induced by the excitation of the CdSeS crown, the CdSe core was pumped by 450 nm fs pulses. To minimize nonradiative Auger recombination, low pumping power was selected to excite the CdSe core ($N = 0.05$, N is the average number of exciton per nanoparticles). CdSe and CdSe/CdSeS NPLs exhibit ground-state bleaching (GSB) signals around 512 nm under 450 nm pulse excitation, consistent with their steady-state absorption. Figure 3(b) shows the normalized recovery curves of CdSe and CdSe/CdSeS NPLs within 1500 ps. It can be seen that the recovery curves of CdSe and CdSe/CdSeS NPLs have similar values at 0 and 1500 ps, but their decay processes differ. The time constants obtained through biexponential function fitting of the fs-TA

data were $\tau_1 = 37.4$ ps and $\tau_2 = 1049.5$ ps, for the CdSe, and $\tau_1 = 334.1$ ps and $\tau_2 = 6848.1$ ps for CdSe/CdSeS. Here, τ_1 is attributed to the electron trapping, while τ_2 corresponds to exciton relaxation.[27] Compared with CdSe NPLs, the longer τ_1 of CdSe/CdSeS suggests that the electron trapping on the lateral surface of CdSe is passivated by CdSeS crown. Combining the above findings, it can be concluded that both the electron and hole trapping on the lateral surface of CdSe NPLs are passivated by CdSeS crown, leading to an increase in PLQY and a shorter PL lifetime.

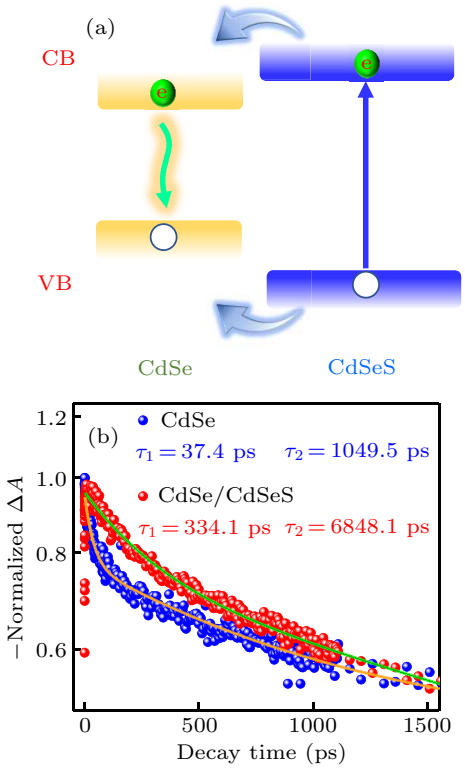


Fig. 3. (a) The electronic structure of CdSe/CdSeS core/crown NPLs. (b) Ultrafast carrier dynamic of CdSe and CdSe/CdSeS NPLs.

The enhanced optical performance of CdSe NPLs due to electron and hole defect passivation prompted us to investigate their differences in optical gain. Specifically, the CdSe and CdSe/CdSeS NPLs solution was drop-cast onto a quartz plate to form a dense solid film. To pump the NPLs, a 355 nm laser beam with a 1 ns pulse width and 20 Hz repetition rate was focused onto the film using a cylindrical lens (focal length: 7.5 cm).[28] The emission was collected from the side surface and detected by a CCD. Figures 4(a) and 4(b) show the power-dependent emission spectra of CdSe and CdSe/CdSeS NPLs, respectively. It was found that at low excitation density, the emission spectrum was dominated by a broad spontaneous emission with FWHM of around 16 nm. In addition, it is found that the emission peak of the NPLs exhibits a noticeable redshift relative to the PL peak shown in Fig. 2(a), which is attributed to the biexciton emission due to the large biexciton binding energy of the 4 ML CdSe NPLs.[29] With the increase of the excitation density, a sharp peak with a FWHM of 6 nm appears on the low-energy side of the NPLs emission, indicating the onset of ASE.[30] This also confirms that the optical gain of CdSe/CdSeS NPLs originates from biexcitons.[31] The emission intensity as a function of the excitation density is shown in the inset. The ASE thresholds of CdSe and CdSe/CdSeS NPLs are calibrated to be 0.75 and 0.16 mJ/cm^2, respectively. CdSe/CdSeS NPLs exhibit a lower ASE threshold than CdSe due to the passivation of electron and hole trapping on the lateral surface of CdSe. According to our previous studies, the improved optical gain due to surface passivation can be attributed to the increase in absorption cross-section and Auger recombination lifetime.[32] Therefore, NPLs with fewer surface defects are more likely to achieve population inversion. Compared to the CdSe/CdZnS core/shell structure, the larger threshold of CdSe/CdSeS core/crown NPLs may be related to differences in test conditions and sample structures.[33] Importantly, it was demonstrated for the first time that CdSe/CdSeS core/crown NPLs can achieve ASE under nanosecond pulse pumping.

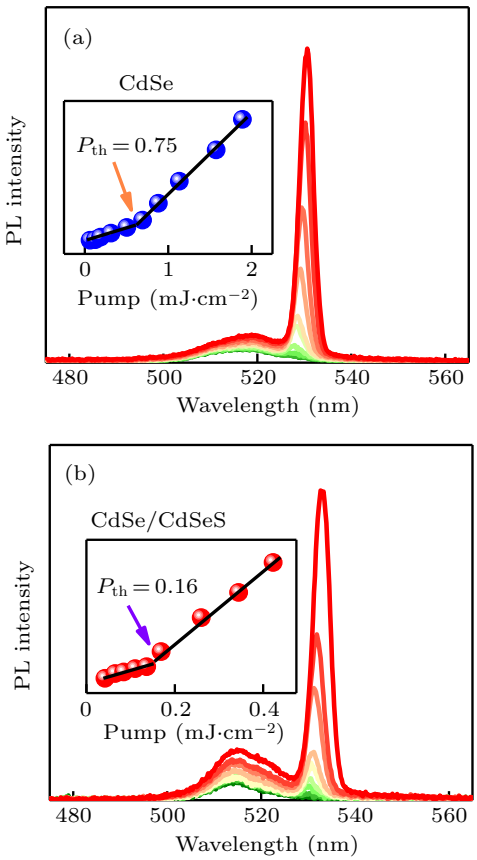


Fig. 4. Pump-power dependence of ASE: (a) CdSe, (b) CdSe/CdSeS. The inset is the pump power dependence integrated PL intensity.

Benefiting from the superior optical gain properties of CdSe/CdSeS NPLs and the strong scattering properties of "photonic glass", random lasers may be realized from CdSe/CdSeS NPLs/SiO_2 composite films.[34] In order to verify the hypothesis, CdSe/CdSeS NPLs were drop-cast onto a

quartz wafer containing SiO_2 microspheres (around 20 μm) to form CdSe/CdSeS NPLs/SiO_2 composite films.[2] The composite films were pumped by a nanosecond laser (optical wavelength: 355 nm; pulse: 1 ns; and repetition rate: 20 Hz). Similar to the ASE, the lasing signals of CdSe/CdSeS NPLs were detected by a spectrometer. The emission spectra at different pump densities are shown in Fig. 5(a). It can be seen that under low-power pump density, the emission of CdSe/CdSeS NPLs/SiO_2 is primarily spontaneous emission. As the power increases, sharp emission peaks appear (with FWHM < 1 nm) at the shoulder of the stimulated emission, indicating that the lasing behavior is achieved in the CdSe/CdSeS NPLs.[4,35] In addition, it is found that the spacing between the lasing peaks is not fixed, which can confirm the generation of random lasing.[32] The integrated emission intensity as a function of pump power is shown in Fig. 5(b). The nonlinear increase in emission intensity indicates the formation of a random laser. The threshold for random laser was measured at 0.21 mJ/cm^2.

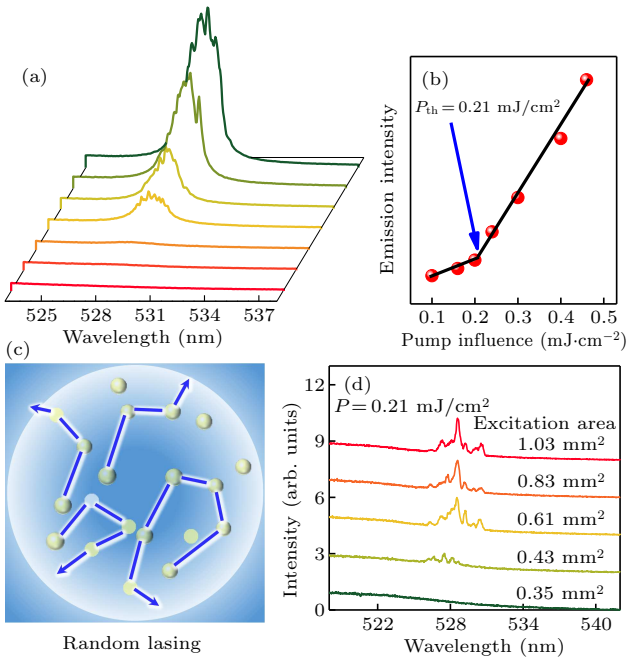


Fig. 5. (a) Pump power dependent emission spectra from CdSe/CdSeS NPLs. (b) Pump power dependent integrated PL intensity of CdSe/CdSeS NPLs. (c) Schematic of coherent random lasing from CdSe/CdSeS/SiO_2. (d) Area-dependent emission spectra of random lasing.

According to the random laser theory, random lasers can be classified into two types: coherent and incoherent.[36,37] Incoherent random lasers typically have a spectrum centered around the gain maximum and a linewidth of several nanometers.[36] Coherent random lasers, on the other hand, are composed of multiple scattering loops, as illustrated in Fig. 5(c). The spectrum of coherent random lasing usually consists of multiple lasing peaks.[37] Based on this characteristic, the random laser generated from the CdSe/CdSeS NPLs/SiO_2 thin film can be classified as a coherent random laser. In addition, more lasing modes are formed with the increase of pump power, which results from different thresholds of the random cavities. To further confirm the coherent random lasing action, the pump area dependence was characterized, as shown in Fig. 5(d).[32] At low pump area, the space is too small to form scattering loops. As the pumping area increases, more scattering loops are formed, leading to a higher number of emitted modes. Therefore, as the excitation area increases, the modes of random lasing increase. Based on this, the random laser generated by the CdSe/CdSeS/SiO_2 is confirmed to be a coherent random laser.

4. Conclusion

In conclusion, we constructed a coherent random laser pumped by nanosecond pulses using high-gain CdSe/CdSeS NPLs and high scattering SiO_2 microspheres. CdSe/CdSeS NPLs exhibit higher emission efficiency and faster PL lifetime than bare-core CdSe due to the electron and hole trapping on the lateral surfaces being passivated by CdSeS. Due to surface passivation, the ASE threshold of CdSe decreases from 0.75 to 0.16 mJ/cm^2 for CdSe/CdSeS NPLs. The pump area-dependent emission spectrum confirms the generation of coherent random lasing. Our results lay the foundation for surface passivation engineering and multifunctional device applications of CdSe NPLs.

Acknowledgements

The authors acknowledge the assistance of SUSTech Core Research Facilities. This work is supported by the National Natural Science Foundation of China (Grant No. 62174079), Guangdong Provincial Quantum Science Strategic Initiative (Grant No. GDZX2404006), Science, Technology and Innovation Commission of Shenzhen Municipality (Grant No. JCYJ20220530113015035).

References

[1] Zhang D G, Jian L Y, Tseng Z L, Cheng H M and Lin J H 2021 *Nanoscale* **13** 3246
[2] Li X, Wang Y, Sun H and Zeng H 2017 *Adv. Mater.* **29** 1701185
[3] Meng B, Zhang X, Kang Y, Yu X, Wang P, Wang S, Tang J, Hao Q, Wei Z and Chen R 2024 *Nanoscale* **16** 17488
[4] Yang J, Liu Z, Pi M, Lin H, Zeng F, Bian Y, Shi T, Du J, Leng Y and Tang X 2020 *Adv. Opt. Mater.* **8** 2000290
[5] Padiyakkuth N, Thomas S, Antoine R and Kalarikkal N 2022 *Mater. Adv.* **3** 6687
[6] Sapienza R 2022 *Nat. Phys.* **18** 976
[7] Liu H, Hao J, Li J, Cheng J, Gao Y, Lin X, Wang K and He T 2020 *J. Phys. Chem. C* **124** 27840
[8] Zhang L, Yang H, Yu B, Tang Y, Zhang C, Wang X, Xiao M, Cui Y and Zhang J 2020 *Adv. Opt. Mater.* **8** 1901615
[9] Liu H, Lin D, Wang P, He T and Chen R 2024 *Chip* **3** 100073
[10] Pietryga J M, Park Y S, Lim J, Fidler A F, Bae W K, Brovelli S and Klimov V I 2016 *Chem. Rev.* **116** 10513
[11] Diroll B T, Guzelturk B, Po H, Dabard C, Fu N, Makke L, Lhuillier E and Ithurria S 2023 *Chem. Rev.* **123** 3543
[12] Liu H, Chen P, Cui Y, Gao Y, Cheng J, He T and Chen R 2023 *Adv. Opt. Mater.* **11** 2300425
[13] Park Y S, Bae W K, Baker T, Lim J and Klimov V I 2015 *Nano Lett.* **15** 7319

[14] Park Y S, Bae W K, Padilha L A, Pietryga J M and Klimov V I 2014 *Nano Lett.* **14** 396
[15] Wu K, Lim J and Klimov V I 2017 *ACS Nano* **11** 8437
[16] Gao Y, Liu H, Li J, Deng X, Hu W, Xiao S, Qiu X, Lin X, Wang K and He T 2020 *J. Phys. Chem. C* **124** 7994
[17] Lo S S, Mirkovic T, Chuang C H, Burda C and Scholes G D 2011 *Adv. Mater.* **23** 180
[18] Liu H, Chen P, Zhang X, Wang X, He T and Chen R 2023 *Nanoscale* **15** 14140
[19] Hu A, Bai P, Zhu Y, Song Z, Wang R, Zheng J, Yao Y, Zhang Q, Ding Z, Gao P, Sui X, Liu X and Gao Y 2022 *Adv. Opt. Mater.* **10** 2200469
[20] Duan R, Zhang Q, Thung Y T, Zhou X, Yin T, Ao Y, Xiao L, Zhang Z, Lee C X X, Ren T, Demir H V, Lew W S, Zhang B and Sun H 2025 *Adv. Mater.* **37** 2416635
[21] Yu J, Zhang C, Pang G, Sun X W and Chen R 2019 *ACS Appl. Mater. Interfaces* **11** 41821
[22] Dufour M, Qu J, Greboval C, Méthivier C, Lhuillier E and Ithurria S 2019 *ACS Nano* **13** 5326
[23] Prudnikau A, Chuvilin A and Artemyev M 2013 *J. Am. Chem. Soc.* **135** 14476
[24] Coropceanu I, Rossinelli A, Caram J R, Freyria F S and Bawendi M G 2016 *ACS Nano* **10** 3295
[25] Purcell-Milton F, Visheratina A K, Kuznetsova V A, Ryan A, Orlova A O and Gun'ko Y K 2017 *ACS Nano* **11** 9207
[26] Liu H, Wang P, Huang Z, Wang S, Ren Z, Liu J, He T and Chen R 2025 *J. Phys. Chem. Lett.* **16** 1567
[27] Yang W, Yang Y, Kaledin A L, He S, Jin T, McBride J R and Lian T 2020 *Chem. Sci.* **11** 5779
[28] Wang Y, Li X, Zhao X, Xiao L, Zeng H and Sun H 2016 *Nano Lett.* **16** 448
[29] Grim J Q, Christodoulou S, Di Stasio F, Krahne R, Cingolani R, Manna L and Moreels I 2014 *Nat. Nanotechnol.* **9** 891
[30] Guzelturk B, Kelestemur Y, Olutas M, Delikanli S and Demir H V 2014 *ACS Nano* **8** 6599
[31] Li M, Zhi M, Zhu H, Wu W Y, Xu Q H, Jhon M H and Chan Y 2015 *Nat. Commun.* **6** 8513
[32] Wang Y, Ta V D, Gao Y, He T C, Chen R, Mutlugun E, Demir H V and Sun H D 2014 *Adv. Mater.* **26** 2954
[33] Duan R, Zhang Z, Xiao L, Zhao X, Thung Y T, Ding L, Liu Z, Yang J, Ta V D and Sun H 2022 *Adv. Mater.* **34** 2108884
[34] Ye L, Niu D, Lu C, Gu B and Xu S 2025 *Opt. Laser Technol.* **182** 112124
[35] Lin W, Wang C, Tong B, Sun B, Zhao X and Gao Y 2023 *Mater. Lett.* **349** 134789
[36] Cao H 2003 *Waves Random Media* **13** R1
[37] Cerdan L, Enciso E, Martin V, Banuelos J, Lopez-Arbeloa I, Costela A and Garcia-Moreno I 2012 *Nat. Photon.* **6** 621